

Mass composition of cosmic rays with energy above 10^{17} eV according to the data of surface detectors of Yakutsk EAS array

A. V. Sabourov*, A. V. Glushkov, M. I. Pravdin, Yu. A. Egorov, A. A. Ivanov,
S. P. Knurenko, V. P. Mokhnachevskaya, I. S. Petrov, L. V. Timofeev

Yu. G. Shafer Institute of cosmophysical research and aeronomy SB RAS

E-mail: tema@ikfia.ysn.ru

In this paper we present our estimation of mass composition of cosmic rays with energy above 10^{17} eV. It was obtained from the analysis of the lateral distribution of cascade particles in extensive air showers registered at the Yakutsk EAS array over the course of continuous observations from 1974 to 2017. Experimental values were compared to simulation results obtained within the framework of four hadron interaction models. The result of this comparison shows that over the energy range $(1 - 20) \times 10^{17}$ eV cosmic rays mass composition changes from nuclei with $\langle \ln A \rangle \simeq 2.5$ to protons.

*35th International Cosmic Ray Conference — ICRC2017
10–20 July, 2017
Bexco, Busan, Korea*

*Speaker.

1. Introduction

Mass composition of cosmic rays (CR) with energy (E_0) above $\sim 10^{17}$ eV is still not known precisely, despite of being thoroughly investigated for more than 40 years at the world's extensive air shower (EAS) arrays [1]. The Yakutsk EAS array provides multi-component air showers registration, so we have several composition-sensitive parameters to choose from. They include muon fraction in charged particles and parameters of the lateral distribution function (LDF) of Cherenkov light, but also it is possible to estimate the CR mass composition by analyzing the LDF of particles registered by surface scintillation detectors (SSD) (see e.g. [2–6]).

The most common technique is based on studying the features of the air shower longitudinal development, by estimating or measuring the depth of maximum shower development (x_{\max}) which is tied to the atomic number of primary nuclei with a simple relation:

$$\ln A = \frac{x_{\max}^p - x_{\max}^{\text{exp.}}}{x_{\max}^p - x_{\max}^{\text{Fe}}} \cdot \ln 56, \quad (1.1)$$

where values denoted with ‘exp.’ are obtained experimentally; and p and Fe — are obtained theoretically, usually via air shower simulations for primary protons and iron nuclei. Earlier we have calculated LDFs of the Yakutsk EAS array's SSD response (see [7–9]) in showers with $E_0 \geq 10^{17}$ eV. This result was obtained in simulations with CORSIKA code [10] with the use of four hadron interaction models — QGSJet01D [11], QGSJet-II-04 [12], SIBYLL-2.1 [13] and EPOS-LHC [14]. FLUKA code [15] was used for low-energy interactions. Here we compare these LDFs with experimental data collected during the period of continuous observations from 1974 to 2017.

2. Events selection and data processing

For the analysis we selected events with $\theta \lesssim 45^\circ$ ($\langle \cos \theta \rangle = 0.9$) and selected data from only 13 stations located near the center of the array. With central station they form 6 triggering (master) triangles with 500 m side (small master, SM, or trigger-500) and 1000 m (large master, LM, or trigger-1000). These stations contain two scintillation detectors (2×2 m² each) operating in 2- μ s coincidence mode. Preliminary energy values were estimated according to empirical relations [16]:

$$E_0 = (4.8 \pm 1.6) \times 10^{17} \cdot \rho_{s,600}(0^\circ)^{1.0 \pm 0.02} \text{ (eV)}, \quad (2.1)$$

$$\rho_{s,600}(0^\circ) = \rho_{s,600}(\theta) \cdot \exp\left(\frac{1020 \cdot (\sec \theta - 1)}{\lambda}\right) \text{ (m}^2\text{)}, \quad (2.2)$$

$$\lambda = (450 \pm 44) + (32 \pm 15) \cdot \log_{10} \rho_{s,600}(0^\circ) \text{ (g/cm}^2\text{)}, \quad (2.3)$$

where $\rho_{s,600}(\theta)$ is the particle density at $r = 600$ m from shower axis measured by SSD. Geometry reconstruction is performed with the LDF based on Linsley approximation:

$$f_s(r, \theta) = \rho_{s,600}(\theta) \cdot \left(\frac{600 + r_1}{r + r_1}\right)^a \cdot \left(\frac{600 + r_M}{r + r_M}\right)^{b-a}, \quad (2.4)$$

where $a = 1$, $r_1 = 0$, r_M — is the Moliere radius which depends on air temperature t (measured in $^\circ\text{C}$) and pressure p (in mbar):

$$r_M = \frac{7.5 \times 10^4}{p} \cdot \frac{t + 273}{273} \text{ (m)}. \quad (2.5)$$

The r_M value is estimated in every individual event (for Yakutsk $\langle t \rangle \simeq -18^\circ\text{C}$, $\langle r_M \rangle \simeq 70$ m). The b parameter in (2.4) was determined earlier as

$$b = 1.38 + 2.16 \cdot \cos \theta + 0.15 \cdot \log_{10} \rho_{s,600}(\theta). \quad (2.6)$$

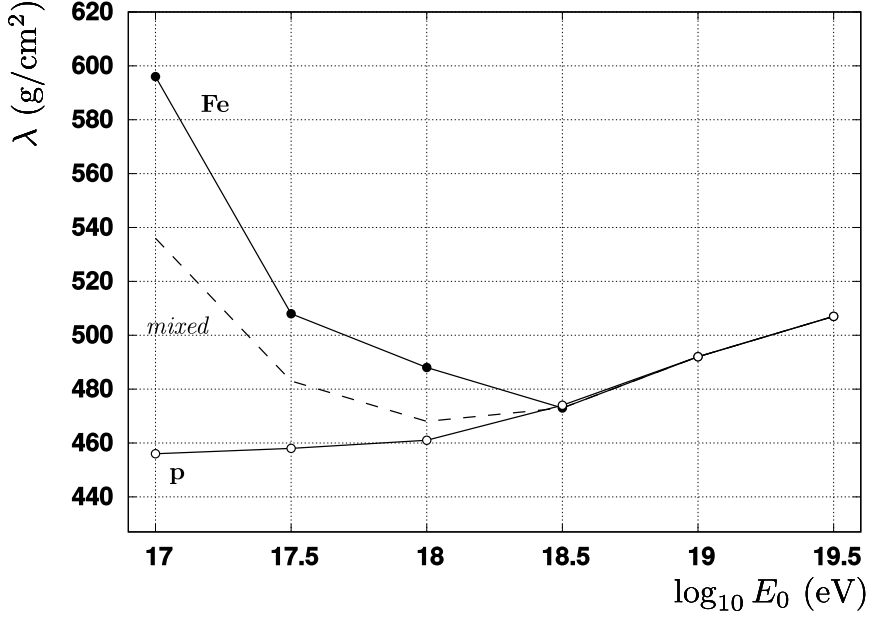


Figure 1: Energy (E_0) dependence of the absorption range λ in (2.2) when $\rho_{s,600}(\theta)$ is recalculated to vertical arrival direction. Simulation within the framework of QGSJet01d model for primary protons (p), mixed composition and primary iron nuclei (Fe).

The final analysis includes showers with axes localizes with uncertainties not exceeding 20-30 m for trigger-500 and 50 m — for trigger-1000. Mean LDFs were constructed in logarithmic bins $h = \Delta \log_{10} E_0 = 0.2$ with step $0.5h$. When constructing the mean LDFs the values of particle density in individual showers were multiplied by normalizing ratio $\langle E_0 \rangle / E_0$, where $\langle E_0 \rangle$ is the mean energy for a group. Then these values were averaged in radial bins with logarithmic step $\Delta \log_{10} r = 0.4$. Average particle densities were determined as

$$\langle \rho_s(r_i) \rangle = \frac{1}{N} \sum_{k=1}^N \rho_k(r_i), \quad (2.7)$$

where N is the number of detector's indications within a radial interval $(\log_{10} r_i, \log_{10} r_i + 0.4)$. Resulting LDFs were fitted with the following function:

$$\rho_s(r, \theta) = f_s(r, \theta) \cdot \left(\frac{600 + r_2}{r + r_2} \right)^{10}, \quad (2.8)$$

where $a = 2$, $r_M = 10$, $r_1 = 8$ and $r_2 = 10^4$ m. Here r_M became a formal parameter. In conjunction with other parameters of approximation (2.8), it provides the best agreement with density values

obtained with (2.7) in all range of shower axis distance (30 – 2000) m. The best fit values of $\rho_{s,600}(\theta)$ and b in individual groups of events were obtained with χ^2 test. Final values of primary energy E_0 for resulting mean LDFs were obtained according to the refined calorimetric formula [9]:

$$E_0 = (3.76 \pm 0.3) \times 10^{17} \cdot \rho_{s,600}(0^\circ)^{1.02 \pm 0.02} \text{ (eV)}, \quad (2.9)$$

with absorption range λ shown on Fig. 1.

3. Primary mass composition

3.1 The shape of lateral distribution

The b parameter reflects the steepness of the LDF which is sensitive to the mass composition. Its values obtained with the relation (2.8) are shown on Fig. 2 with dark circles. Lines represent expected values according to different hadron interaction models [9].

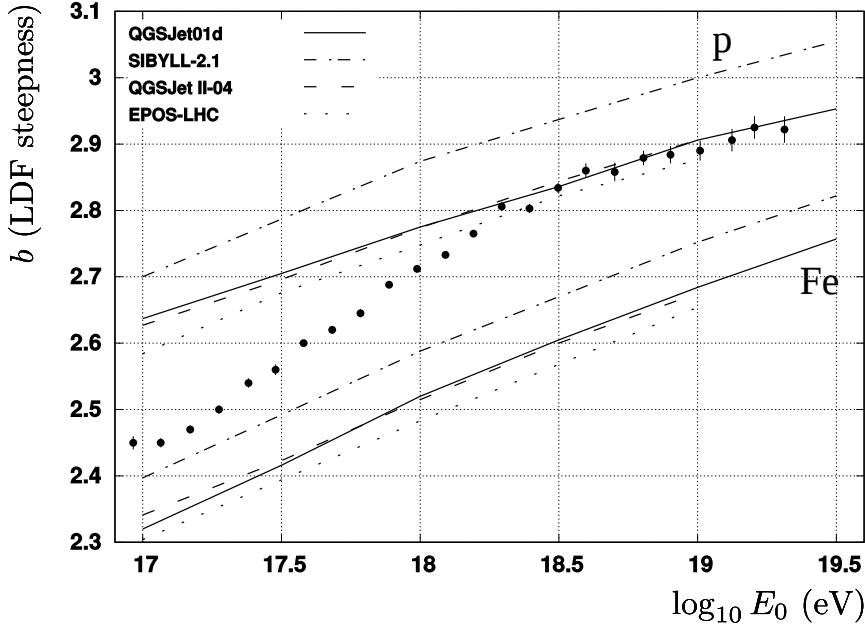


Figure 2: The steepness parameter of the LDF of detector response in the axis distance range 30-2000 m in showers with $\cos \theta = 0.9$ with different primary energy. Lines represent simulations with different hadron interaction models for protons and iron nuclei, symbols — experimental values.

All models except for SIBYLL-2.1 gave similar results which do not contradict the experiment. They allow to estimate the composition of primary particles from the relation

$$\langle \ln A \rangle = w_p \cdot \ln 1 + w_{Fe} \cdot \ln 56, \quad (3.1)$$

where $w_p = 1 - w_{Fe}$, $w_{Fe} = \langle \ln A \rangle / \ln 56$. Since

$$w_{Fe} = \frac{d_{\text{exp.}} - d_p}{d_{Fe} - d_p}, \quad (3.2)$$

where $d = b$, the values obtained in the experiment (exp) and predicted in simulations (p, Fe), the final relation has the following form:

$$\langle \ln A \rangle = \frac{d_{\text{exp}} - d_p}{d_{\text{Fe}} - d_p} \cdot \ln 56. \quad (3.3)$$

The results obtained within the framework of QGSJet01D model are shown on Fig. 3. At energy $\sim 10^{17}$ eV it agrees with the data of KASCADE [17] and Tunka-133 (QGSJet-II-04) [18].

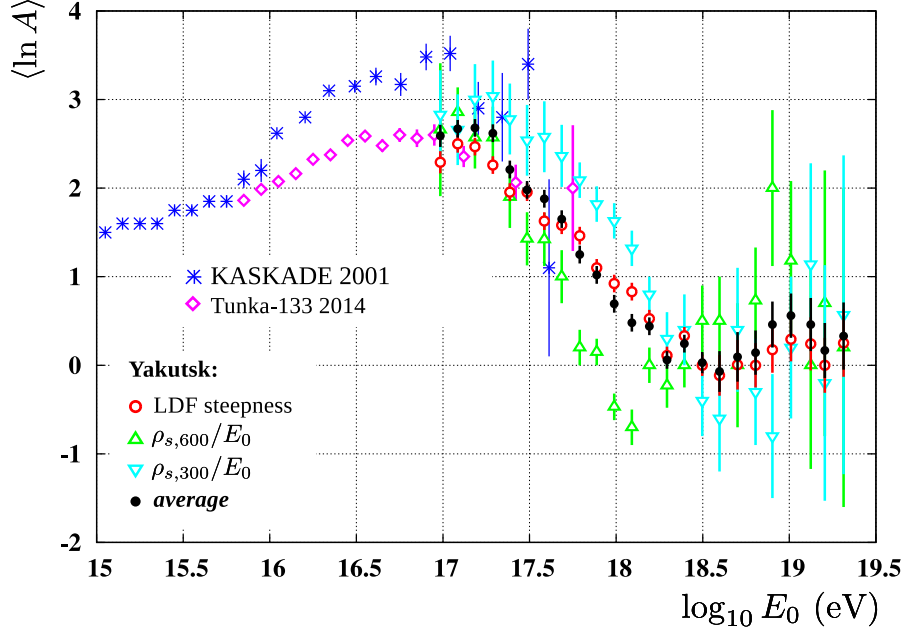


Figure 3: Energy dependence of primary CR composition obtained at the Yakutsk array from the LDF steepness parameters and from ratios $\rho_{s,600}/E_0$ and $\rho_{s,300}/E_0$ (see below). Other symbols represent the data of KASCADE [17] and Tunka-133 [18].

3.2 Absolute values of lateral distribution

Simulations have indicated that density values at axis distance $r = 460$ m ($\rho_{s,460}$) are proportional to E_0 at any given CR composition, i.e. LDFs of showers with the same energy would inter-cross. This fact provides the possibility to choose *the* hadron interaction model. On Fig. 4 (b) are shown normalized values $\rho_{s,460}/E_0$ for all four models. In our case, the experimental data show the best agreement with the QGSJet01D model.

On Fig. 4 (a) and 4 (c) are shown normalized densities $\rho_{s,600}/E_0$ and $\rho_{s,300}$ which are easily derivable from experimental data but are more sensitive to CR composition than the $\rho_{s,460}/E_0$. From relations (3.1) and (3.2) with $d = \log_{10} \rho_{s,600}/E_0$ and $d = \log_{10} \rho_{s,300}/E_0$ for the QGSJet01D model, we obtained estimation of the CR mass composition which is shown on Fig. 3 with triangles. On the same plot with dark circles are shown our average estimates.

The estimated CR mass composition obtained at the Yakutsk array from different EAS components is shown on Fig. 5 [19–21]. On the same plot are shown estimations of the $\langle \ln A \rangle$ at energy above 10^{18} eV that follow from the data of The Pierre Auger Observatory (PAO) [22] and The Telescope Array Project (TA) [23].

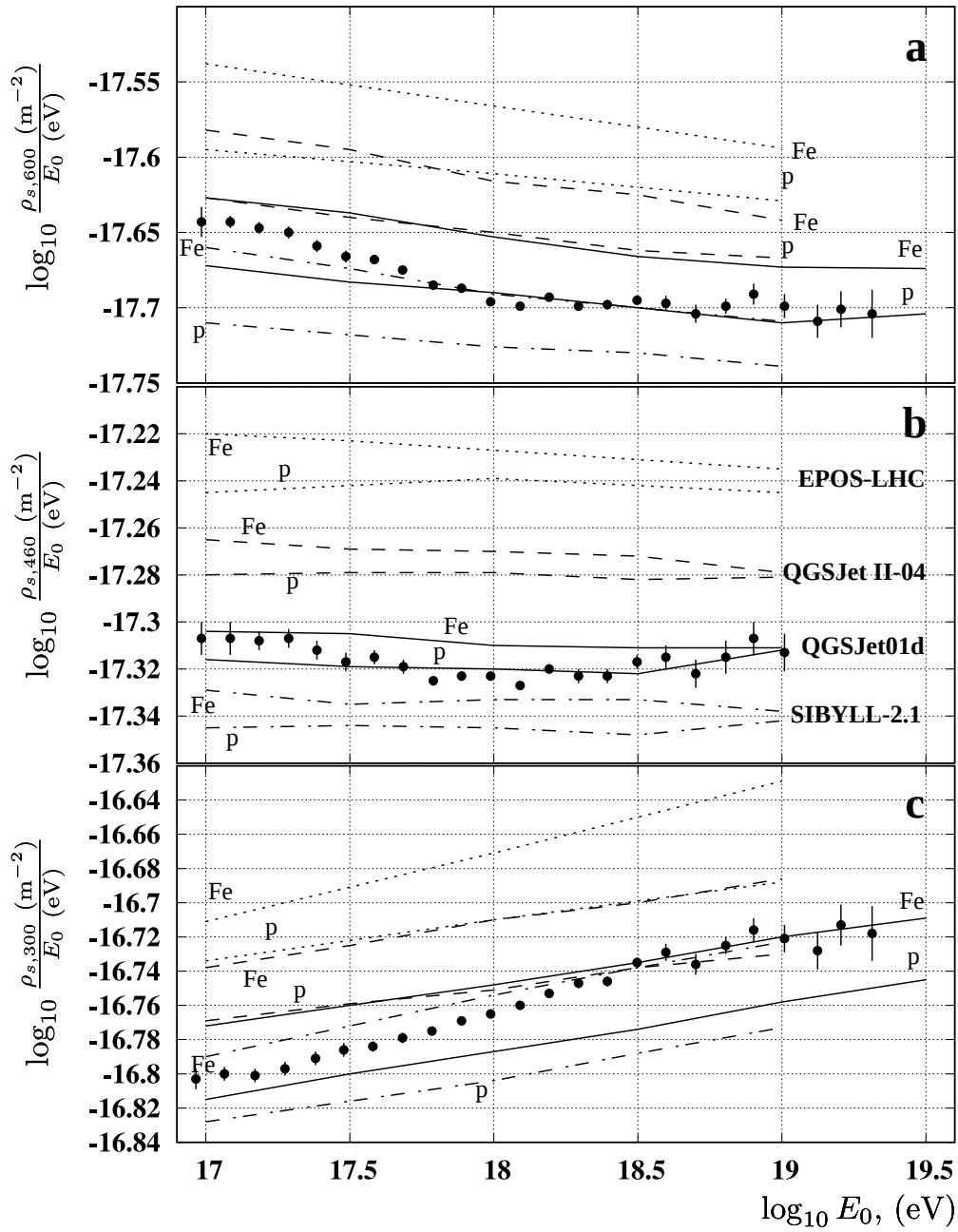


Figure 4: Particle densities measured by SSD at $r = 600$ m (a), $r = 460$ m (b) and 300 m (c) from shower axis. Lines represent theoretical predictions, symbols — experimental values.

The data shown above demonstrate that the Yakutsk EAS array provides the basis for a complex analysis of the CR mass composition within the widest possible energy range. The results of this analysis, within measurement errors, show a good agreement between each other and with the data of world experiments.

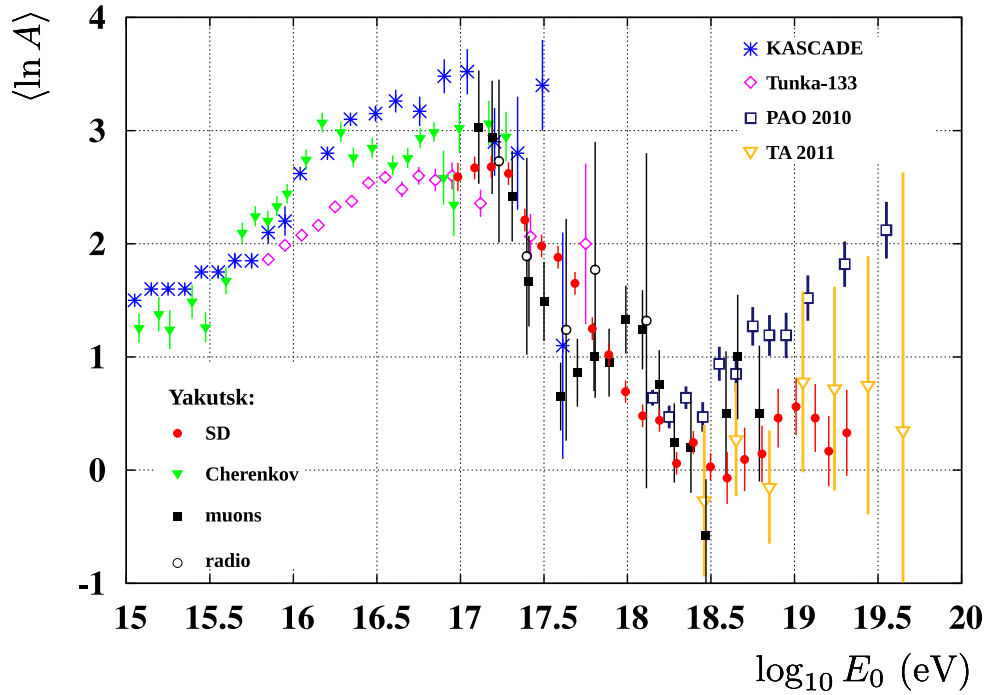


Figure 5: Energy dependence of CR mass composition according to various world experiments.

4. Conclusion

Long term measurement of lateral distribution of particles in extensive air showers registered at the Yakutsk array and its comparison to simulation results provided the opportunity to estimate CR mass composition in the energy range $10^{17} - 10^{18}$ eV. It is evident from the Fig. 5 that the composition changes with energy in $(1 - 20) \times 10^{17}$ eV towards lighter nuclei. It is quite possible that this change arises from the transition from galactic CR component to extragalactic. Based on the data presented on the Fig. 3 one may conclude that at energy above $\sim 2 \times 10^{17}$ eV primary cosmic rays consist of pure protons. However there is not enough evidence yet for such a strict conclusion. Here we need further study which we plan to continue.

The work is supported by the program of Presidium of RAS "High-energy physics and neutrino astronomy" and by RFBR grant 16-29-13019 ofi-m.

References

- [1] P. K. F. Grieder. *Extensive Air Showers: High Energy Phenomena and Astrophysical Aspects — A Tutorial, Reference Manual and Data Book*. Springer Berlin Heidelberg, 2010, [10.1007/978-3-540-76941-5](https://doi.org/10.1007/978-3-540-76941-5).
- [2] A. V. Glushkov, PhD thesis, SINP MSU, Moscow, 1982. (in Russian)
- [3] A. V. Glushkov, L. G. Dedenko, N. N. Efimov, N. N. Efremov, I. T. Makarov, P. D. Petrov et al. *Bull. Acad. Sci. USSR Phys.* **50** (1986) 2166–2167. (in Russian)
- [4] A. V. Glushkov, M. I. Pravdin, I. E. Sleptsov, V. R. Sleptsova and N. N. Kalmykov, *Phys. At. Nucl.* **63** (2000) 1477–1488.

- [5] A. V. Glushkov and A. V. Sabourov, *JETP Lett.* **98** (2014) 589–592.
- [6] E. G. Berezhko, S. P. Knurenko and L. T. Ksenofontov, *Astropart. Phys.* **36** (2012) 31–36.
- [7] A. V. Glushkov, M. I. Pravdin and A. V. Sabourov, *JETP Lett.* **99** (2014) 431–434.
- [8] A. V. Glushkov, M. I. Pravdin and A. Sabourov, *Phys. Rev. D* **90** (Jul, 2014) 012005.
- [9] A. V. Glushkov, Y. A. Egorov, A. A. Ivanov, S. P. Knurenko, V. P. Mokhnachevskaya, I. S. Petrov et al. *Proc. of 35th ICRC*, PoS(ICRC2017)552, (Busan, Korea), 2017.
- [10] D. Heck, J. Knapp, J. N. Capdevielle, G. Schatz and T. Thouw, **FZKA 6019**, Forschungszentrum Karlsruhe, 1988.
- [11] N. N. Kalmykov, S. S. Ostapchenko and A. I. Pavlov, *Nucl. Phys. B (Proc. Suppl.)* **52** (1997) 17–28.
- [12] S. Ostapchenko, *Phys. Rev. D* **83** (2011) 014018, [[arXiv:1010.1869](https://arxiv.org/abs/1010.1869)].
- [13] E.-J. Ahn, R. Engel, T. K. Gaisser, P. Lipari and T. Stanev, *Phys. Rev. D* **80** (2009) 094003, [[arXiv:0906.4113](https://arxiv.org/abs/0906.4113)].
- [14] T. Pierog, I. Karpenko, J. M. Katzy, E. Yatsenko and K. Werner, [[arXiv:1306.0121](https://arxiv.org/abs/1306.0121)] (2013).
- [15] G. Battistoni, S. Muraro, P. R. Sala, F. Cerutti, A. Ferrari et al. *Proc. of the Hadronic Shower Simulation Workshop 2006*, vol. 896, pp. 31–49, 2007.
- [16] B. N. Afanasiev, B. N. Dyakonov, T. A. Egorov et al. *Proc. of the Tokyo Workshop on Techniques for the Study of Extremely High Energy Cosmic Rays*, pp. 35–51, 1993.
- [17] H. Ulrich, T. Antoni, W. D. Apel, F. Badea, K. Bekk, A. Bercuci et al. *Proc. of the 27th ICRC, Hamburg, Germany*, vol. 1, p. 97, 2001.
- [18] V. V. Prosin, S. F. Berezhnev, N. M. Budnev, A. Chiavassa, O. A. Chvalaev et al. *Nucl. Instr. Meth. A* **756** (2014) 94 – 101.
- [19] A. A. Ivanov, S. P. Knurenko, A. A. Lagutin, M. I. Pravdin, A. V. Sabourov and I. E. Sleptsov, *Bull. Russ. Acad. Sci. Phys.* **71** (2007) 448–450.
- [20] A. V. Glushkov and A. V. Sabourov, *JETP* **119** (2014) 848–853.
- [21] S. Knurenko, I. Petrov, Z. Petrov and I. Sleptsov, *Proc. of 34th ICRC*, PoS(ICRC2015)254, (The Hague, The Netherlands), 2015.
- [22] S. Andringa for THE PIERRE AUGER OBSERVATORY collaboration, *Results of the Pierre Auger Observatory on Astroparticle Physics*, [[arXiv:1005.3795](https://arxiv.org/abs/1005.3795)] (2010).
- [23] Y. Tsunesada for TELESCOPE ARRAY collaboration, *Highlights from Telescope Array*, [[arXiv:1111.2507v1](https://arxiv.org/abs/1111.2507v1)] (2011).